TAMPERE UNIVERSITY OF TECHNOLOGY

Complex Double-Binary-Offset-Carrier modulation for a unitary characterization of Galileo and GPS signals

Elena Simona Lohan, Abdelmonaem Lakhzouri, and Markku Renfors

Institute of Communications Engineering, Tampere University of Technology

P.O. Box 553, FIN-33101, Finland,

Tel: +358 3 3115 3915, Fax: +358 3 3115 3808

elena-simona.lohan@tut.fi, abdelmonaem.lakhzouri@unav-micro.fi,

markku.renfors@tut.fi

Abstract

In this paper we introduce a new class of modulations, the Complex Double Binary-Carrier-Offset (CDBOC) modulation class, which covers most of the modulation types proposed so far for Galileo and GPS signals, namely the binary and quaternary phase shift keying (BPSK/QPSK), sine BOC (SinBOC), cosine BOC (CosBOC) and alternate BOC (AltBOC) modulations. At the same time, CDBOC class provides a more general framework, with potential for new applications of wide-band CDMA systems and/or future satellite navigation systems. We introduce the theoretical derivations of the Power Spectral Density (PSD) and the Auto-Correlation Function (ACF) of the CDBOC-modulated signals, and we compare the theoretical analysis with the results obtained via simulations. The advantage of our method in the context of Galileo and GPS signals is its simplicity and the fact that it provides unified analytical formulas for most of the existent GPS/Galileo signals.

I. INTRODUCTION

The modulation type used for basic GPS signals, such as C/A and P(Y) codes, is the Binary Phase Shift Keying (BPSK) modulation [1]. Other signals in L1-band of GPS and Galileo, e.g.,

GPS M-code, Open-Services (OS) and Publicly-Regulated-Services (PRS) signals, use a sine or cosine Binary-Offset-Carrier (BOC) modulation, described in [2], [3], [4], [5]. The specifications for L5 GPS signals and the proposals for E5 Galileo signals include QPSK and Alternative BOC (AltBOC) modulations [6], [7], [8], [9]. The main properties of the modulated waveforms are related to the the autocorrelation shapes, which determine the acquisition and tracking abilities, and to the spectral content (i.e., PSD), which determines the bandwidth consumption and the spectral separation with other signals sharing the same spectrum. The properties of the classical BPSK and QPSK modulations are typically well-known and understood, but those of the BOC-modulation families are still a topic of active research. Currently, to the authors' knowledge, there is no unified analysis of various BOC-modulation classes (e.g., SinBOC, CosBOC, AltBOC) and the theoretical formulas available for the ACF and PSD of these families are typically given for particular cases. For example, theoretical formulas for the PSD are given in [2] for SinBOC signals and in [4] for CosBOC of even modulation orders only. The ACF functions for SinBOC and CosBOC signals are typically based on simulations [2], [5], [7] or on prototyping[1] rather than on theoretical modelling. More recently, the authors have developed the idea of real Double-BOC (DBOC) modulation, which covers the classes of BPSK, sine BOC and cosine BOC modulations [11]. However, the analysis there [11] was focused on the spectral separation between existing GPS signals and potential Galileo signals. Moreover, QPSK and AltBOC signals were not taken into account. For AltBOC signals, only simulations-based ACF and PSD curves are available, e.g. in [6], [7].

A generalization of BOC modulation classes was also proposed in [12], but the approach there is completely different from our approach, it covers only SinBOC and CosBOC modulations, and it provides non-unitary, separate PSD formulas for odd and even modulation orders, as well as for SinBOC and CosBOC cases.

---

[1] One of the first Galileo receivers has been built by Septentrio and ACF shapes based on this receiver have been published in [10].

The goal of this paper is to introduce the concept of the Complex Double Binary-Carrier-Offset (CDBOC) modulation, which will allow a unified analysis of most of the modulation types proposed so far for GPS and Galileo signals[2]. We will show that this new modulation class allows a straightforward and unified theoretical analysis of the time and spectral properties of the modulated signals. The analysis introduced here is useful not only for the current Galileo proposals, but may find its applications for the future satellite navigation signals and for other wideband CDMA-based communication and navigation systems.

II. COMPLEX DOUBLE BINARY-CARRIER-OFFSET (CDBOC) CONCEPT

In order to introduce the Complex-Double-BOC concept, we start from the sine and cosine BOC modulation waveforms. BOC modulation is a square sub-carrier modulation, where a signal is multiplied by a rectangular sub-carrier of frequency f_{sc}, which splits the spectrum of the signal into two parts [2], [3]. Typically, the sine and cosine BOC modulations are defined via two parameters $\text{BOC}(m_{BOC}, n_{BOC})$ [2], related to the reference 1.023 MHz frequency as follows: $m_{BOC} = f_{sc}/1.023$ and $n_{BOC} = f_c/1.023$, where f_c is the chip rate (both f_{sc} and f_c are expressed in MHz here). From the point of view of the equivalent baseband signal, the SinBOC and CosBOC modulations can be defined via a single parameter (as it will be shown below), denoted in what follows by BOC modulation order N_1:

$$N_1 \triangleq 2\frac{m_{BOC}}{n_{BOC}} = 2\frac{f_{sc}}{f_c}. \tag{1}$$

Any sine or cosine BOC-modulated (Sin/CosBOC) signal $x(t)$ can be seen as the convolution

---

[2] Exceptions are the optimized Galileo signals proposed in [13]

between a Sin/CosBOC waveform $s_{Sin/CosBOC}(t)$ and a modulating waveform $d(t)$, as follows:

$$
\begin{aligned}
x(t) &= \sum_{n=-\infty}^{+\infty} d^{(n)} \sum_{k=1}^{S_F} c^{(n,k)} s_{Sin/CosBOC}(t - nT_{sym} - kT_c) \\
&= s_{SinBOC}(t) \circledast \sum_{n=-\infty}^{+\infty} \sum_{k=1}^{S_F} d^{(n)} c^{(n,k)} \delta(t - nT_{sym} \\
&\quad - kT_c) \triangleq s_{Sin/CosBOC}(t) \circledast d(t),
\end{aligned}
\tag{2}
$$

where $\circledast$ is the convolution operator, $d(t)$ is the data sequence to be spread (defined above), $d^{(n)}$ is the complex data symbol corresponding to the n-th code symbol (for example, in case of a pilot channel, $d^{(n)} = 1, \forall\, n$, and, typically, $d^{(n)}$ is constant over a large range of code symbols n, because the data symbol rates are much smaller than the code symbol rates in GPS and Galileo [14], [15]), T_{sym} is the code symbol period[3], $c_{k,n}$ is the $k-$th chip corresponding to the $n-$th symbol, $T_c = 1/f_c$ is the chip period, S_F is the spreading factor ($S_F = T_{sym}/T_c$), and $\delta(t)$ is the Dirac pulse. In order to derive the expression of eq. (2), we used the Dirac property: $s(t) = s(t) \circledast \delta(t), \forall$ signal $s(t)$. In eq. (2), we assumed to have wideband data, i.e., spread via a pseudorandom (PRN) sequence, because the signals used in GPS and Galileo are wideband signals. However, the model holds also for narrowband data.

The SinBOC $s_{SinBOC}(t)$ and CosBOC $s_{CosBOC}(t)$ waveforms used in eq. (2), have two equivalent definitions given in eqs. (3) and (4), respectively (the equivalence between the two definitions can be proved via simulations and, also, by reasoning; eq. (3) has been introduced in [2])

$$
\begin{cases}
s_{SinBOC(m_{BOC},n_{BOC})}(t) & \triangleq sign\left(sin\left(\frac{N_1 \pi t}{T_c} \right) \right), \\
& 0 \le t < T_c \\
s_{CosBOC(m_{BOC},n_{BOC})}(t) & \triangleq sign\left(cos\left(\frac{N_1 \pi t}{T_c} \right) \right), \\
& 0 \le t < T_c
\end{cases}
\tag{3}
$$

---

[3] We remark that the code symbol terminology used here is not necessarily synonymous with the code epoch; the code symbol is defined by the spreading factor via $S_F = T_{sym}/T_c$, while the code epoch is defined by the ranging code repetition period [15]. For example, for GPS C/A signal, the code symbol period is equal to the code epoch interval of 1 ms and $S_F = 1023$, while for Galileo OS signals, the code epoch length is set to 4092 chips, while the code repetition period and, thus, the spreading factor, are still to be defined (values of $S_F = 1023$ and $S_F = 4092$ have been proposed so far).

and, equivalently,

$$
\begin{cases}
s_{SinBOC(m_{BOC},n_{BOC})}(t) &= p_{T_{B_1}}(t) \circledast \sum_{i=0}^{N_1-1} (-1)^i \\
&\qquad \delta(t - iT_{B_1}),\ 0 \le t < T_c \\
s_{CosBOC(m_{BOC},n_{BOC})}(t) &= p_{\frac{T_{B_1}}{2}}(t) \circledast \sum_{i=0}^{N_1-1} \sum_{k=0}^{1} (-1)^{i+k} \\
&\qquad \delta\left(t - iT_{B_1} - \frac{kT_{B_1}}{2}\right), \\
&\qquad 0 \le t < T_c
\end{cases}
\tag{4}
$$

where $sign(\cdot)$ is the signum operator, N_1 is the BOC-modulation order defined in eq. (1), and $p_{T_{B_1}}(\cdot)$ is the rectangular pulse of amplitude 1 and support $T_{B_1} = T_c/N_1$, i.e., a pulse defined via

$$
p_{T_{B_1}}(t) \triangleq
\begin{cases}
1 & \text{if } 0 \le t < T_{B_1}, \\
0 & \text{otherwise}
\end{cases}
\tag{5}
$$

We remark that both right-hand and left-hand terms of equalities in eq. (4) are sequences of ± 1, with support in $[0, T_c)$, since the pulses added in the right-hand sides of eq. (4) are non-overlapping in time domain.

By looking at the limits of the sums in eq. (4), we can straightforwardly define the concept of real Double-BOC (DBOC) modulation waveform, of orders N_1 and N_2, and chip rate f_c:

$$
s_{DBOC(N_1,N_2,f_c)}(t) = p_{T_{B_{12}}}(t) \circledast \sum_{i=0}^{N_1-1} \sum_{k=0}^{N_2-1} (-1)^{i+k} \delta\Big(t - iT_{B_1} \\
- kT_{B_{12}}\Big),\ 0 \le t < T_c,
\tag{6}
$$

where $T_{B_{12}} = T_c/(N_1 N_2)$. It follows that SinBOC and CosBOC modulations are only particular cases of the real DBOC modulation, when $N_2 = 1$ and $N_2 = 2$, respectively. The real DBOC modulation can be seen (somehow) as a two-stage SinBOC modulation[4], which justifies its denomination[5].

---

[4] Indeed, $p_{T_{B_{12}}}(t) \circledast \sum_{i=0}^{N_1-1} \sum_{k=0}^{N_2-1} (-1)^{i+k} \delta\Big(t - iT_{B_1} - kT_{B_{12}}\Big) = p_{T_{B_{12}}}(t) \circledast \sum_{i=0}^{N_1-1} (-1)^i \delta\Big(t - iT_{B_1}\Big) \circledast \sum_{k=0}^{N_2-1} (-1)^k \delta\Big(t - kT_{B_{12}}\Big)$.

[5] For example, the classical notation SinBOC(1,1) [2] will correspond to DBOC(2,1,1.023 MHz)

Now, let $x_u(t) = x_{u,re}(t) + jx_{u,im}(t)$, $u = 1, 2$ be two (real[6] or complex) signals, where each $x_{u,v}(t)$ signal, $u = 1, 2$, $v = re, im$, has been obtained by spreading a data sequence (with symbols $d_{u,v}^{(n)}$, not necessarily binary) via a pseudorandom code sequence (with chips $c_{u,v}^{(n,k)}$):

$$x_{u,v}(t) = \sum_{n=-\infty}^{\infty} d_{u,v}^{(n)} \sum_{k=1}^{S_F} c_{u,v}^{(n,k)} \delta(t - nT_{sym} - kT_c), \tag{7}$$

where T_{sym} is the symbol period, T_c is the chip interval, S_F is the spreading factor ($S_F = T_{sym}/T_c$), n is the symbol index, and k is the chip index. In what follows, $x_i(t)$, $i = 1, 2$, will be the modulating signals. Let N_1, N_2, N_3, and N_4 be four positive integer numbers, satisfying the condition that $N_3 N_4$ is a divisor[7] of $N_1 N_2$ (i.e., $N_1 N_2/(N_3 N_4) \triangleq P_{res} \in \mathbb{N}$).

The CDBOC-modulated signal $y_{CDBOC}(t)$, which uses (in quadrature) the modulating signals $x_1(t)$ and $x_2(t)$, is built as follows:

$$
\begin{aligned}
y_{CDBOC(N_1,N_2,N_3,N_4,f_c)}(t) &= x_1(t) \circledast p_{T_{B_{12}}}(t) \circledast \sum_{i=0}^{N_1-1} \\
&\sum_{k=0}^{N_2-1} (-1)^{i+k} \delta\left(t - iT_{B_1} - kT_{B_{12}}\right) \\
&+ jx_2(t) \circledast p_{T_{B_{12}}}(t) \circledast \sum_{l=0}^{N_3-1} \sum_{m=0}^{N_4-1} \sum_{p=0}^{P_{res}-1} (-1)^{l+m} \\
&\delta\left(t - iT_{B_3} - mT_{B_{34}} - pT_{B_{12}}\right),
\end{aligned}
\tag{8}
$$

where $T_{B_i} = T_c/(N_i)$ and $T_{B_{34}} = T_c/(N_3 N_4)$. The block diagram of the CDBOC[8] modulation is shown in Fig. 1. The summation of P_{res} terms of the quadrature term of eq. (8) (and, thus, the hold block of Fig. 1) is due to the need of equal sub-chip rates for the in-phase and quadrature components (e.g., the sub-sample interval after DBOC(N_1, N_2) processing is equal to $T_c/(N_1 N_2)$, while the sub-sample interval after DBOC(N_3, N_4) processing is equal to $T_c/(N_3 N_4)$; thus, the

---

[6] If the signal $x_u(t)$ is real, this is modeled via zero imaginary part: $x_{u,im}(t) = 0$.

[7] The situation when $N_1 N_2$ is a divisor of $N_3 N_4$ can be treated similarly.

[8] The CDBOC modulation is, hence, defined via 5 parameters, namely 4 CDBOC modulation orders and the chip rate: CDBOC(N_1, N_2, N_3, N_4, f_c). However, from the point of view of the baseband signals, f_c can be ignored. In what follows, we will sometimes also use the notations CDBOC(N_1, N_2, N_3, N_4) (when the chip rate does not affect the results) or CDBOC, for simplicity.

higher sub-sample rate between the two branches in Fig. 1 is P_{res} higher than the lower rate and a hold block is needed to bring the two branches of Fig. 1 at equal rates). The in-phase $x_1(t)$ and quadrature $x_2(t)$ modulating signals can be either equal or distinct. For each branch, DBOC modulation is applied, thus forming a complex signal which is sent to the channel.

It can be easily seen that most of the modulations proposed so far for GPS and Galileo signals, namely BPSK, SinBOC, CosBOC, QPSK and AltBOC, are only particular cases of the CDBOC-modulation, as shown in Table I.

In Table I, the factor a is the ratio between the chip rate f_c and the reference GPS chip rate 1.023 MHz. The sign '$-$' stands for 'don't care' values. We remark that AltBOC signals can be either with constant envelope or with non-constant envelope, and the envelope properties are defined by the choice of the signals $x_1(t)$ and $x_2(t)$ (i.e., binary or non-binary, real or complex, equal or distinct). A description of the choice of $x_1(t)$ and $x_2(t)$ signals for various AltBOC types can be found in [7] and is out the scope of this paper. In what follows, we will show that the power spectral densities for various modulating signals will mainly depend on whether the signals $x_1(t)$ and $x_2(t)$ are equal or distinct.

III. THEORETICAL DERIVATIONS OF ACF AND PSD

The ACF, $\mathcal{R}_{CDBOC}(\tau)$, of the CDBOC-modulated waveform can be derived starting from eq. (8) and from its definition[9]:

$$\mathcal{R}_{CDBOC}(\tau) \triangleq \mathbf{E}\big(y_{CDBOC}(\tau) \circledast y_{CDBOC}(\tau)\big)$$
$$= \mathbf{E}\bigg(\int_{-\infty}^{\infty} y_{CDBOC}^*(\tau - t) y_{CDBOC}(t) dt\bigg) \qquad (9)$$

where $\mathbf{E}(\cdot)$ is the expectation operator (with respect to the random parameters, i.e., PRN codes and data sequences), and * is the conjugate operator. If we assume ideal spreading code properties

[9] Indeed, since we deal with a random signal waveform with time-variation, the ACF should be given as the expectation of the time autocorrelation of $y_{CDBOC}(\cdot)$ signal, and the time auto-correlation of $y_{CDBOC}(\cdot)$ is the convolution between the signal and the conjugate of its mirror image.

(i.e., $\mathcal{R}_{x_{u,v}}(\tau) = \delta(\tau)$) and independent real and imaginary parts of the modulating signals $x_{u,v}(t)$, $u = 1, 2$, we obtain, after several manipulations, the followings:

$$
\begin{cases}
\text{If } x_1(t) \neq x_2(t), \ \mathcal{R}_{CDBOC}(\tau) = \mathcal{R}_1(\tau) + \mathcal{R}_2(\tau) \\
\text{If } x_1(t) = x_2(t), \ \mathcal{R}_{CDBOC}(\tau) = \mathcal{R}_1(\tau) + \mathcal{R}_2(\tau) \\
\qquad\qquad\qquad\qquad\qquad\quad + 2j\mathcal{R}_{12}(\tau),
\end{cases} \tag{10}
$$

where

$$
\begin{cases}
\mathcal{R}_1(\tau) = \sum_{i=0}^{N_1-1}\sum_{k=0}^{N_2-1}\sum_{i_1=0}^{N_1-1}\sum_{k_1=0}^{N_2-1} (-1)^{i+i_1+k+k_1}\Lambda_{T_B}\Big(\tau \\
\qquad\qquad - (i-i_1)T_{B_1} - (k-k_1)T_{B_{12}}\Big), \\[2mm]
\mathcal{R}_2(\tau) = \sum_{l=0}^{N_3-1}\sum_{m=0}^{N_4-1}\sum_{l_1=0}^{N_3-1}\sum_{m_1=0}^{N_4-1}\sum_{p=0}^{N_{res}-1}\sum_{p_1=0}^{N_{res}-1} \\
\qquad\qquad (-1)^{l+l_1+m+m_1}\Lambda_{T_B}\Big(\tau - (l-l_1)T_{B_3} \\
\qquad\qquad - (m-m_1)T_{B_{34}} - (p-p_1)T_{B_{12}}\Big), \\[2mm]
\mathcal{R}_{12}(\tau) = \sum_{i=0}^{N_1-1}\sum_{k=0}^{N_2-1}\sum_{l=0}^{N_3-1}\sum_{m=0}^{N_4-1}\sum_{p=0}^{N_{res}-1} \\
\qquad\qquad (-1)^{i+k+l+m}\Lambda_{T_B}\Big(\tau - iT_{B_1} + lT_{B_3} - kT_{B_{12}} \\
\qquad + \ mT_{B_{34}} + pT_{B_{12}}\Big)
\end{cases} \tag{11}
$$

Above, $\Lambda_{T_B}(t)$ is the triangular pulse of support $2T_{B_{12}}$ and centered at 0. Eq. (11) is valid for non-zero modulating signals. If one of the modulating signals is zero, e.g., $x_2(t) = 0$, then $\mathcal{R}_{CDBOC}(\tau) = \mathcal{R}_1(\tau)$.

Despite their rather heavy appearance, the expressions given in eq. (11) are simply additions of delayed triangular pulses, and can be easily implemented with reduced complexity. Examples will be shown in Section IV.

The PSD of CDBOC signal is the Fourier transform of the ACF. We distinguish again two

cases:

$$
\begin{cases}
\text{If } x_1(t) = x_2(t): & \mathcal{S}_{CDBOC}(f) = \frac{1}{T_c} S_{X_1}(f)|H(f)|^2 \\[2mm]
\text{If } x_1(t) \neq x_2(t): & \mathcal{S}_{CDBOC}(f) = \frac{1}{T_c}\left(S_{X_1}(f)| \right. \\[2mm]
& \left. H_{upper}(f)|^2 + S_{X_2}(f)|H_{lower}(f)|^2 \right)
\end{cases}
\tag{12}
$$

where $\mathcal{S}_{CDBOC}(f)$ is the PSD of the CDBOC-modulated signal and $S_{X_i}(f)$ is the PSD of the (random) modulating data $x_i(t)$, $i = 1, 2$. The normalization with $1/T_c$ factor is done in order to have unity signal power over infinite bandwidth, similar with the definitions in [2]. Above, $H(f)$ is the equivalent transfer function of the block diagram shown in Fig. 1, $H_{upper}(f)$ is the transfer function of upper branch in Fig. 1, and $H_{lower}(f)$ is the transfer function of lower branch in Fig. 1. If the modulating signals are distinct, then they are assumed to be independent. Based on Fig. 1 and eq. (8),

$$
H(f) = P_{T_{B_{12}}}(f)H_{12}(f) + P_{T_{B_{12}}}(f)H_{34}(f)H_{hold}(f),
\tag{13}
$$

where $P_{T_{B_{12}}}(f) = T_{B_{12}} sinc(fT_{B_{12}})$ is the Fourier transform of a rectangular pulse (here $sinc(x) \triangleq sin(\pi x)/(\pi x)$), $H_{12}(f)$ is the transfer function of the DBOC(N_1, N_2) modulation of Fig. 1:

$$
\begin{aligned}
H_{12}(f) &= \sum_{i=0}^{N_1-1}\sum_{k=0}^{N_2-1} (-1)^{i+k} e^{j2\pi f(iT_{B_1}+kT_{B_{12}})} \\
&= \left(\frac{1-(-1)^{N_1}e^{-j2\pi fT_c}}{1+e^{-j2\pi fT_{B_1}}} \right) \left(\frac{1-(-1)^{N_2}e^{-j2\pi fT_{B_1}}}{1+e^{-j2\pi fT_{B_{12}}}} \right),
\end{aligned}
\tag{14}
$$

$H_{34}(f)$ is obtained similarly with $H_{12}(f)$[10], by replacing 1 with 3 and 2 with 4, and $H_{hold}(f)$ is the transfer function of the hold block of Fig. 1:

$$
H_{hold}(f) = \sum_{p=0}^{P_{res}-1} e^{j2\pi f(pT_{B_{12}})} = \left(\frac{1-e^{-j2\pi fT_c}}{1-e^{-j2\pi fT_{B_{12}}}} \right).
\tag{15}
$$

Furthermore,

$$
\begin{aligned}
H_{upper}(f) &= P_{T_{B_{12}}}(f)H_{12}(f) \\
H_{lower}(f) &= P_{T_{B_{12}}}(f)H_{34}(f)H_{hold}(f).
\end{aligned}
\tag{16}
$$

---

[10] For the derivations of eq. (14), we used the fact that $\sum_{i=0}^{N-1} x^i = \frac{1-x^N}{1-x}$.

By replacing in eq. (12) the expressions given in eqs. (13) to (16), we get the final expressions of the PSD for CDBOC modulated waveforms.

The PSD will clearly depend on the PSD of the input sequences $S_{X_i}(f)$, $i = 1, 2$. However, under the simplifying assumption that $x_i(t)$ sequences are built of zero-mean and uncorrelated chips, $S_{X_i}(f)$ are constant and equal to the sequence power, and, therefore, they do not influence the shape of the output PSD.

IV. COMPARISON BETWEEN THEORY AND SIMULATIONS

The shapes of the ACF for a CDBOC$(3, 2, 3, 1)$ with distinct modulating signals is shown in Fig. 2. These shapes are identical with the ACF for AltBOC(15,10), as explained in Table I. The codes for the simulation results were pseudorandom codes of spreading factors $S_F = 1023$ (m-sequences) and 10230 (Gold sequences). We observe a very close match between theory and simulations. The same match was observed for all the tested signals. We remark that, for ACF curves, the chip rate f_c is not specified in the CDBOC list of parameters, because the ACF curves are not affected by f_c (they are the same for all f_c). On the other hand, the PSD plots depend on f_c as well (not only on CDBOC modulation orders).

For simplicity, in Figs. 3 and 4 we show only the theoretical curves, for 4 distinct CDBOC-modulated signals. The curves from Figs. 3 are for the situation when the same modulating signal $x_1(t)$ is used for the in-phase and quadrature branches. As expected (see eq. (10)), the imaginary part of the ACF in this case is non-zero. A particular case is when the in-phase component uses a CosBOC modulation, and the quadrature component uses a SinBOC modulation, as shown in the left plot of Fig. 3 (this is similar with AltBOC concept, with the difference that the same modulating signal is used for in-phase and quadrature components). Here, the real and imaginary parts carry similar information, but they are delayed from each other with $1/N_1$ chips. The shape of the curves in the left plot of Fig. 3 reminds of the sub-carrier phase cancellation

method proposed in [5] for a non-ambiguous BOC signal acquisition and tracking. Indeed, using a CDBOC($N_1, 2, N_1, 1$) modulation with $x_1(t) = x_2(t)$ will remove the fades in the envelope of the ACF, which are characteristic for SinBOC and CosBOC modulation, and will, therefore, enhance the acquisition performance. This assertion is based on the idea that unambiguous techniques (i.e., techniques which removes the ambiguities in the correlation function, sometimes also called 'BPSK-like' techniques) have better detection probabilities than the ambiguous techniques, as proved in [5], [16], [17], [18].

The plots of Fig. 4 show two CDBOC examples for distinct modulating signals (another example of CDBOC with distinct signals was given before in Fig. 2 for AltBOC(15,10) signals). Here, the imaginary part of the ACF is zero (it carries no information). The left plot corresponds to CosBOC(15,2.5) modulation (as explained in Table I), currently proposed for PRS services [4]. There are typically many fades in the ACF, which should be dealt with for unambiguous tracking of the signals. The right plot of Fig. 4 is a generalized CDBOC(3,4,3,2) signal, which has the possible advantage of better tracking capabilities, due to the wider separation between the main lobe and the adjacent lobes (for example, a High Resolution Correlator [19] or a Very Early-Very Late correlator [3] may be used for tracking the CDBOC signal). The same property of having a narrow main lobe, significantly spaced from the neighbor lobes, can be noticed as well for the new modulation types shown in the right plot of Fig. 3. However, acquisition and tracking algorithms for generic CDBOC waveforms are still to be found.

In terms of PSD, several spectra are shown in Fig. 5. The spectra are not always symmetrical, as seen in the upper left plot of Fig. 5 (when $x_1(t) = x_2(t)$ and CosBOC and SinBOC modulations are used in quadrature, then we have asymmetrical spectrum, as in the upper left plot of Fig. 5). As a general rule, we noticed that AltBOC signals have very similar ACFs and PSDs with SinBOC signals.

V. CONCLUSIONS

The new class of CBDOC-modulated signals allows a generalized and unified framework for the analysis of Galileo and GPS signals. Based on the PSD formulas presented here, various spectral properties, such as the spectral separation coefficients with other GPS/Galileo signals, the root-mean-square bandwidth or the maximum value of the spectrum, can be easily derived and compared. The ACF theoretical curves, derived so far in the absence of channels, can be straightforward extended to multipath channels. The development of new tracking and acquisition algorithms may be based on the theoretical properties of the presented ACF shapes. The extension to various pulse shapes, besides the rectangular one (as included here), is also straightforward, once the transfer function of the filter is known.

ACKNOWLEDGEMENTS

REFERENCES

[1] J. Betz and D. Goldstein, "Candidate Designs for an Additional Civil Signal in GPS Spectral Bands." MITRE Technical Papers, Jan 2002.

[2] J. Betz, "The Offset Carrier Modulation for GPS modernization," in *Proc. of ION Technical meeting*, pp. 639–648, 1999.

[3] B. Barker, J. Betz, J. Clark, J. Correia, J. Gillis, S. Lazar, K. Rehborn, and J. Straton, "Overview of the GPS M Code Signal," in *CDROM Proc. of NMT*, 2000.

[4] G. Hein, M. Irsigler, J. A. Rodriguez, and T. Pany, "Performance of Galileo L1 signal candidates," in *CDROM Proc. of European Navigation Conference GNSS*, May 2004.

[5] V. Heiries, D. Oviras, L. Ries, and V. Calmettes, "Analysis of non ambiguous BOC signal acquisition performance," in *CDROM Proc. of ION GNSS*, (Long Beach, CA), Sep 2004.

[6] L. Ries, L. Lestarquit, E. Armengou-Miret, F. Legrand, W. Vigneau, C. Bourga, P. Erhard, and J. Issler, "A software simulation tool for GNSS2 BOC signals analysis," in *Proc. of ION GPS*, (Portland, OR), pp. 2225–2239, Sep 2002.

[7] L. Ries, F. Legrand, L. Lestarquit, W. Vigneau, and J. Issler, "Tracking and multipath performance assessments of BOC signals using a bit-level signal processing simulator," in *Proc. of ION-GPS2003*, (Portland, OR, US), pp. 1996–2009, Sep 2003.

[8] ARINC, "NAVSTAR GPS Space Segment/Navigation User Interfaces, Interface Specification." IS-GPS-705, ARINC Engineering Services LLC, El Segundo, CA, Nov 2003.

[9] M. Sleewaegen, W. de Wilde, and M. Hollreiser, "Galileo AltBOC receiver," in *CDROM Proc. of ENC GNSS 2004*, (Rotterdam, Netherlands), May 2004.

[10] A. Simsky, J. Sleewaegen, W. de Wilde, and F. Wilms, "Galileo receiver development at Septentrio," in *CDROM Proc. of ENC GNSS 2005*, (Munich, Germany), Jul 2005.

[11] E. Lohan, A. Lakhzouri, and M. Renfors, "A novel family of Binary-Offset-Carrier modulation techniques with applications in satellite navigation systems." submitted to Wiley Journal of Wireless Communications and Mobile Computing.

[12] A. Pratt and J. Owen, "BOC modulation waveforms," in *Proc. of ION-GPS2003*, (Portland, OR, US), pp. 1044–1057, Sep 2003.

[13] G. W. Hein, J. A. Avila-Rodriguez, L. Ries, L. Letarquit, J. L. Issler, J. Godet, and T. Pratt, "A candidate for the Galileo L1 OS optimized signal," in *Proc. of ION-GPS*, (Long Beach, CA), pp. 833–845, Sep 2005.

[14] G. Hein, J. Godet, J. Issler, J. Martin, T. Pratt, and R. Lucas, "Status of Galileo frequency and signal design," in *CDROM Proc. of ION GPS 2002 Meeting*, 2002.

[15] "Galileo joint undertaking (GJU) - Galileo standardization document for 3GPP." GJU web-pages *http://www.galileooju.com* (active Dec 2005), May 2005.

[16] P. Fishman and J. Betz, "Predicting performance of direct acquisition for the M-code signal," in *Proc. of ION NMT*, pp. 574–582, 2000.

[17] N. Martin, V. Leblond, G. Guillotel, and V. Heiries, "BOC(x,y) signal acquisition techniques and performances," in *Proc. of ION-GPS2003*, (Portland, OR, US), pp. 188–198, Sep 2003.

[18] E. S. Lohan, "Statistical analysis of BPSK-like techniques for the acquisition of Galileo signals," in *CDROM Proc. of 23rd AIAA International Communications Satellite Systems Conference (ICSSC)*, Sep 2005.

[19] G. McGraw and M. Braasch, "GNSS multipath mitigation using high resolution correlator concepts," in *in Proc. of ION National Technical Meeting*, (San Diego, CA), pp. 333–342, Jan 1999.
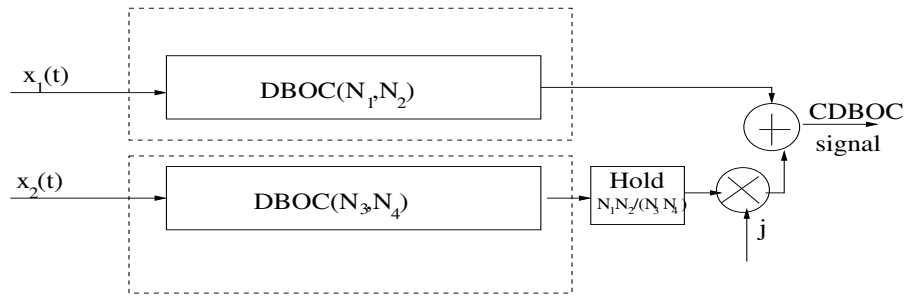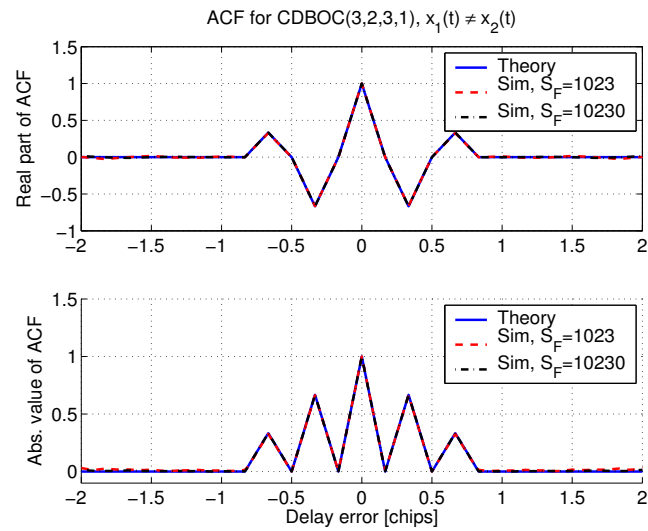
Fig. 1. Block diagram of a CDBOC-modulated signal.

Fig. 2. Autocorrelation functions via theory and via simulations, CDBOC$(3, 2, 3, 1)$, distinct signals.
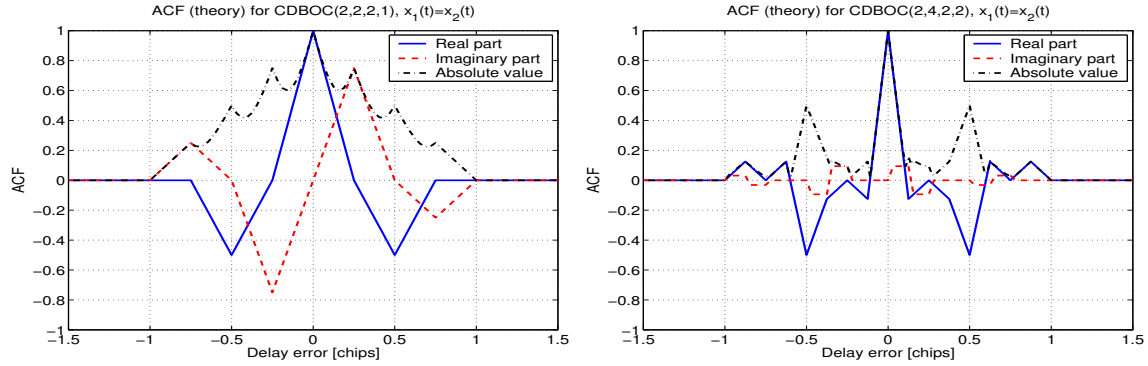
Fig. 3. ACF for various CDBOC waveforms, equal modulating signals.
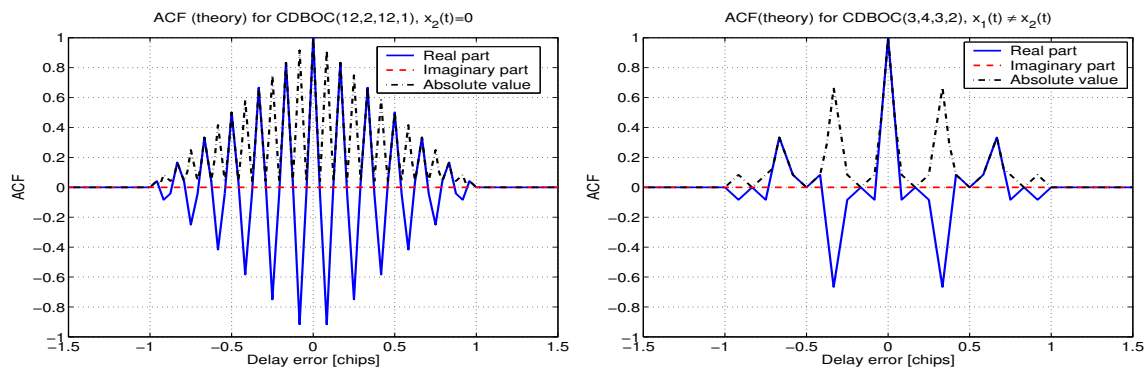

Fig. 4. ACF for various CDBOC waveforms, distinct modulating signals.

TABLE I

THE RELATIONSHIP OF CBDOC-MODULATION FAMILY WITH GPS/GALILEO MODULATION TYPES

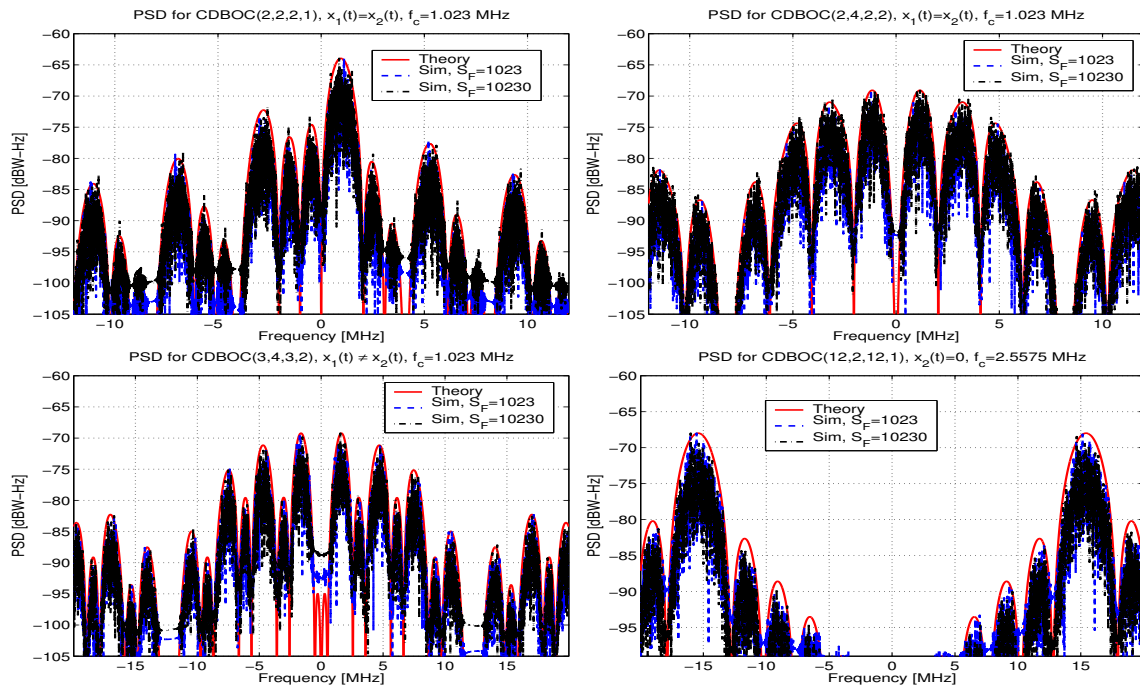| N_1	N_2	N_3	N_4	$x_i(t), i = 1, 2$	Modulation type
1	1	–	–	$x_1(t) =$ binary complex signal $x_2(t) = 0$	BPSK
> 1	1	–	–	$x_1(t) =$ binary complex signal $x_2(t) = 0$	SinBOC$\left(\frac{aN_1}{2}, a\right), a > 0$ (e.g., $a = 1$, $N_1 = 2$, $\Rightarrow$ SinBOC(1,1))
> 1	2	–	–	$x_1(t) =$ binary complex signal $x_2(t) = 0$	CosBOC$\left(\frac{aN_1}{2}, a\right), a > 0$ (e.g., $a = 2.5$, $N_1 = 12$, $\Rightarrow$ CosBOC(15,2.5))
1	1	1	1	$x_1(t), x_2(t)$ distinct binary complex signals	QPSK
> 1	2	$N_3 = N_1$	1	$x_1(t), x_2(t)$ distinct signals	AltBOC$\left(\frac{aN_1}{2}, a\right), a > 0$ (e.g., $a = 10$ and $N_1 = 3$ $\Rightarrow$ AltBOC(15,10))

Fig. 5. PSD for various CDBOC waveforms (theory and simulations).